

# Non-linear oscillation testing of viscoelastic fluids

## *LAOS: Large Amplitude Oscillatory Shear*

Maik Novak, TA Instruments, Germany

Keywords: Non-linear Rheology, LAOS, Harmonics, Intensity ratios

### INTRODUCTION

In an oscillatory experiment a sinusoidal strain or stress is applied to a sample of a material under investigation while measuring the respective answer of the sample. The desired material function is then calculated from the transient signals. This material function is called “modulus” if the stress is related to the strain or “viscosity” in case of the stress being related to the strain rate, whereas the ratio of strain to stress has the character of a “compliance”. Due to the delay between the excitation and the response signals these material functions are generally complex. As sketched in Fig. 1 the transient stress  $\sigma^*$  can be decomposed into an elastic stress  $\sigma'$ , in phase with the deformation  $\gamma$ , and a viscous stress  $\sigma''$ , in phase with the deformation rate  $\dot{\gamma}$ .

### SAOS AND THE LINEAR VISCOELASTIC REGION

Within the so-called linear viscoelastic region (LVR) the response to a sinusoidal excitation is again simply a sinusoid with the same frequency, and moreover the ratio of the amplitudes of input and output signals is independent of the amplitude of the excitation, for example:

$$\frac{|\sigma'|}{|\gamma^*|} = G' = \text{const.} \neq f(|\gamma^*|) \quad (1)$$

From a molecular dynamical view the deformation within the LVR has to be amply small or at least applied sufficiently slowly, that the arrangement of the molecules is never far from a thermodynamic equilibrium; the sample is not altered by the measurement itself. To determine this maximum tolerable, critical deformation is the aim of a so-called strain sweep. A typical result is shown in Fig. 2 for a 4 w% aqueous solution of Xanthan Gum.

During such a strain sweep the amplitude of the angular displacement is increased stepwise at constant frequency, in this case 1 Hz, and the calculated dynamic moduli  $G'$  and  $G''$  are plotted against the strain amplitude. The linear viscoelastic region expands in the shown example up to a strain of about 15 %, characterized by moduli independent of the strain amplitude. The left image Fig. 3 proves that the waveforms of both the excitation (strain) and the response (stress) are simple sinusoids with the same frequency. These two signals that are both drawn with solid lines in Fig. 3 can be differentiated just with the sufficient information, that the stress always advances the strain.

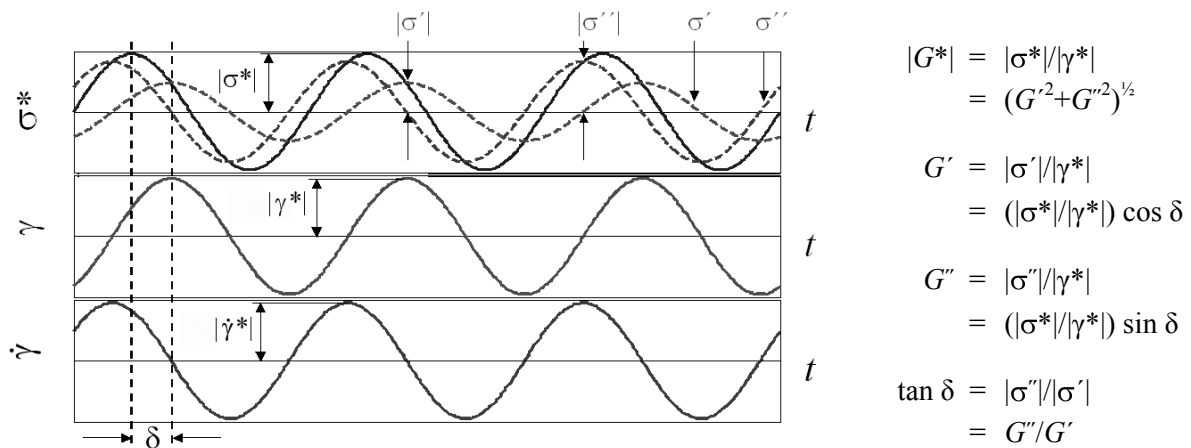


Figure 1: Decomposition of the complex stress into an elastic and a viscous contribution and calculation of the respective moduli

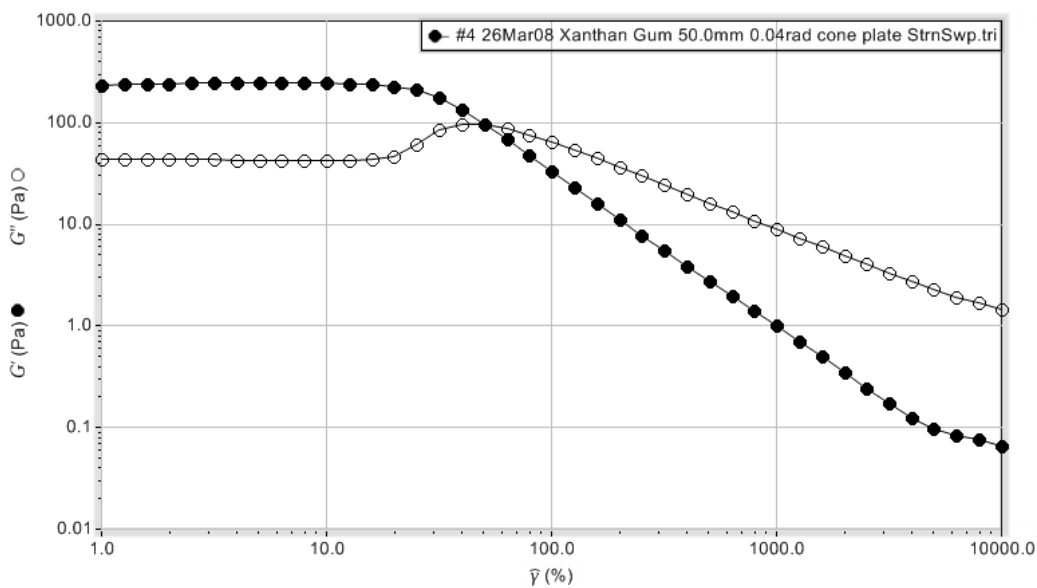


Figure 2: Dynamic moduli obtained from a deformation sweep on a Xanthan Gum solution at constant frequency of 1 Hz. 50 mm-cone/plate system with 0.04 rad.

At larger strains a dependency of the moduli on strain occurs in the given example in such a way, that the storage modulus  $G'$  decreases, whereas the loss modulus  $G''$  first increases and then decreases, like an overshoot phenomenon. In literature this transition from linear to non-linear behavior is termed *Type III* [1]. From the shape of the center and the right waveforms in Fig. 3 it is evident that the material's response to a still sinusoidal excitation cannot be characterized by a sinusoidal function of the same frequency any more; all the quantities that are well known from the linear viscoelastic theory, such as the complex modulus  $|G^*|$ , the storage modulus  $G'$ , the

loss modulus  $G''$  or even the loss factor  $\tan \delta$  loose their physical meaning.

### LAOS and the issue of quantifying non-linear behavior

The stress response of a material to a sinusoidal strain with large amplitude is not only composed of a contribution that oscillates with the excitation frequency, but shows also some higher frequencies, that are invariably integer, neglecting edge effects yet odd multiples of the excitation frequency. There is a quite simple reason for only the odd numbers:

The viscosity of a material can only be an even, symmetric function of the shear rate, as the direction of the deformation has no influence on the resistance against it:

$$\eta(\dot{\gamma}) = a + b \cdot \dot{\gamma}^2 + c \cdot \dot{\gamma}^4 + \dots \quad (2)$$

The shear stress required for this deformation is the product of viscosity and shear rate:

$$\begin{aligned} \sigma(\dot{\gamma}) &= \eta(\dot{\gamma}) \cdot \dot{\gamma} \\ &= (a + b \cdot \dot{\gamma}^2 + c \cdot \dot{\gamma}^4 + \dots) \dot{\gamma} \\ &= a \cdot \dot{\gamma} + b \cdot \dot{\gamma}^3 + c \cdot \dot{\gamma}^5 + \dots \end{aligned} \quad (3)$$

The shear rate in an oscillatory experiment is the derivative of the strain with respect to time:

$$\begin{aligned} \dot{\gamma}(t) &= \frac{d\gamma(t)}{dt} \\ &= \frac{d}{dt} (\gamma^* |\sin \omega t|) \\ &= |\dot{\gamma}^*| \omega \cos \omega t \end{aligned} \quad (4)$$

and substituting (4) in (3) gives for the transient stress

$$\begin{aligned} \sigma(t) &= A \cdot \cos \omega t + B \cdot \cos^3 \omega t \\ &+ C \cdot \cos^5 \omega t + \dots \end{aligned} \quad (5)$$

The only odd powers of the cosines can be converted [2] into

$$\begin{aligned} \cos^3 \omega t &= \frac{1}{4} (3 \cos \omega t + \cos 3\omega t) \\ \cos^5 \omega t &= \frac{1}{16} (10 \cos \omega t + 5 \cos 3\omega t + \cos 5\omega t) \\ \cos^{2N+1} \omega t &= \sum_{n=0}^N c_n \cos(2n+1)\omega t \end{aligned} \quad (6)$$

Substituting in Eq. (5) shows that only odd multiples of the excitation frequency  $\omega$  contribute to the stress response. The magnitudes of these contributions with higher frequencies can be determined by either cross-correlating the stress response against sinusoids with odd multiples of the excitation frequency or directly by a frequency

analysis called Fourier transformation [3 – 5]. The cross-correlation results in discrete values for amplitudes and phase shifts of the higher-frequent contributions, from the Fourier transformation however spectra of these quantities is obtained with more or less distinct maxima of the intensities occurring at the odd multiples of the excitation frequency.

From the ratio of amplitudes of the higher-frequent contributions to the amplitude of the fundamental stress, i. e. that amount of the stress oscillating with the excitation frequency, so-called relative intensities  $I_n/I_1$  of the  $n^{\text{th}}$  harmonic can be derived, that are plotted in Fig. 4. On leaving the LVR by increasing strain amplitude to 15 % at first the relative intensity of the third harmonics (■) increases, at higher strains then also those of the fifth (□), seventh (◆) and ninth (◇) harmonics do. An explanation, e. g. why the relative intensities exhibit a maximum, in order to discuss the material behavior, is at present a matter of research [6 – 10].

Fig. 5 shows further the phase shifts  $\varphi_n$  between the  $n^{\text{th}}$  harmonic and the fundamental stress, plotted as a function of the strain amplitude. Within the LVR such a phase shift is naturally pointless; its definition only acquires a foundation, as soon as the respective higher-frequent contribution has gained a significant intensity.

The following shall attempt to clarify, in which way higher harmonics influence the stress response and especially the shape of their curves in the different means of graphical representation. In order to keep the number of parameters manageable, only the influence of the third harmonic's phase shift  $\varphi_3$  and that of the fundamental  $d_1$  at a fixed relative intensity  $I_3/I_1 = 0.1$  will be discussed. Note: following the proposal of Neidhöfer *et al.* [6]  $\varphi_n$  denotes the phase shift between the  $n^{\text{th}}$  higher harmonics and the fundamental stress, in contrast to the phase shift  $\delta_1$  being the one between funda-

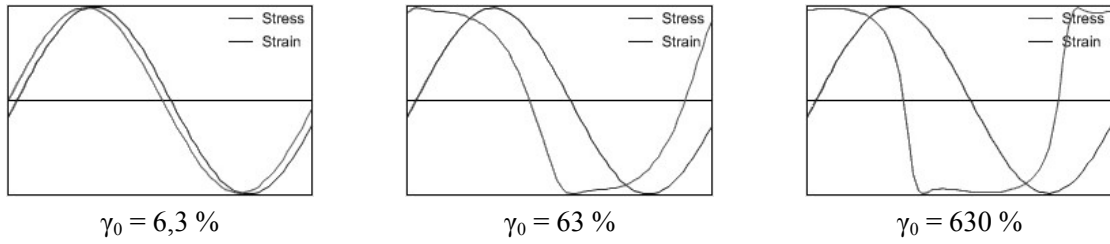


Figure 3: Waveforms of the excitation signal strain and response signal stress during the strain sweep shown in Fig. 2 on Xanthan Gum at different strains

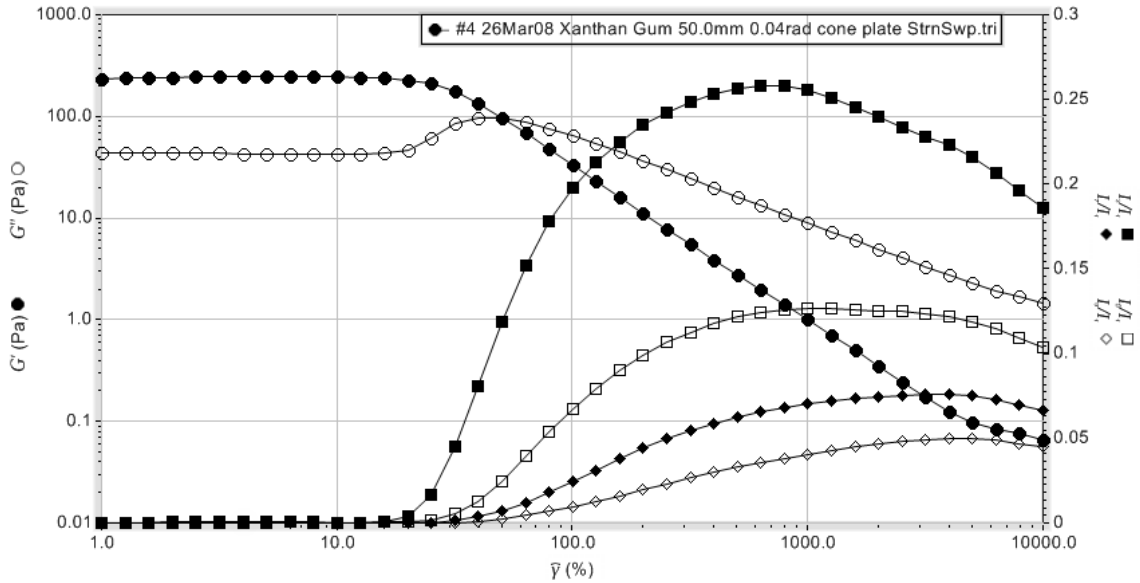


Figure 4: Relative intensities  $I_n/I_1$  of the  $n^{\text{th}}$  harmonics ( $\blacksquare n = 3, \square n = 5, \blacklozenge n = 7, \diamond n = 9$ )

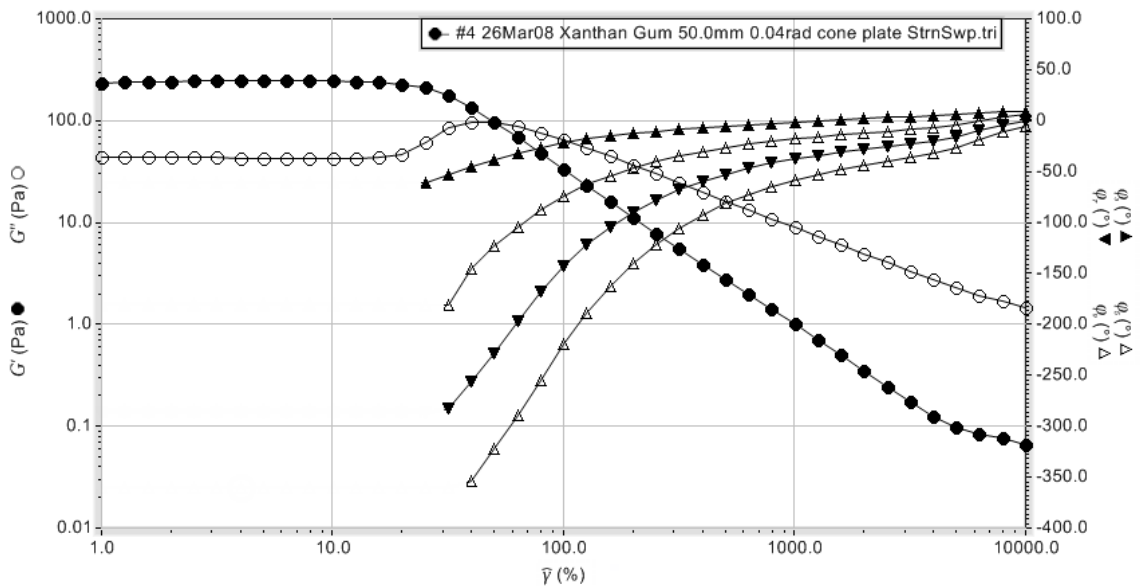


Figure 5: Phase shift  $\varphi_n$  of the  $n^{\text{th}}$  harmonics ( $\blacktriangle n = 3, \triangle n = 5, \blacktriangledown n = 7, \triangledown n = 9$ )

mental stress and the deformation, in exactly the same way as the phase angle  $\delta$ , which is well known from the theory of linear viscoelasticity.

### WAVEFORMS

Fig. 6 shows the waveforms of the stress for  $I_3/I_1 = 0.1$  at various phase shifts  $\delta_1$  of the fundamental and  $\varphi_3$  of the third harmonics versus the time, normalized with the frequency, over one period of oscillation. The open symbols indicate the respective stress contributions, the filled symbols represent the sum of them; both are normalized with the amplitude of the fundamental stress, while the deformation

(solid line) is scaled with the strain amplitude.

Generally the phase angle  $\varphi_3$  lies between  $0^\circ$  and  $360^\circ$ ,  $\delta_1$  however only between  $0^\circ$  and  $90^\circ$ , just as the „viscoelastic phase shift“  $\delta$ . For  $\delta_1 = 0^\circ$  the fundamental stress and the deformation are in-phase; without any third harmonics this was an example of ideally elastic behavior. The occurrence of a third harmonics leads to a change in shape of the stress wave, depending on the value of the phase shift  $\varphi_3$ :

- for  $\varphi_3 = 0^\circ$  the stress wave gets compressed vertically ( $\rightarrow$  square wave)
- for  $\varphi_3 = 90^\circ$  the stress wave gets distorted to the right ( $\rightarrow$  trailing

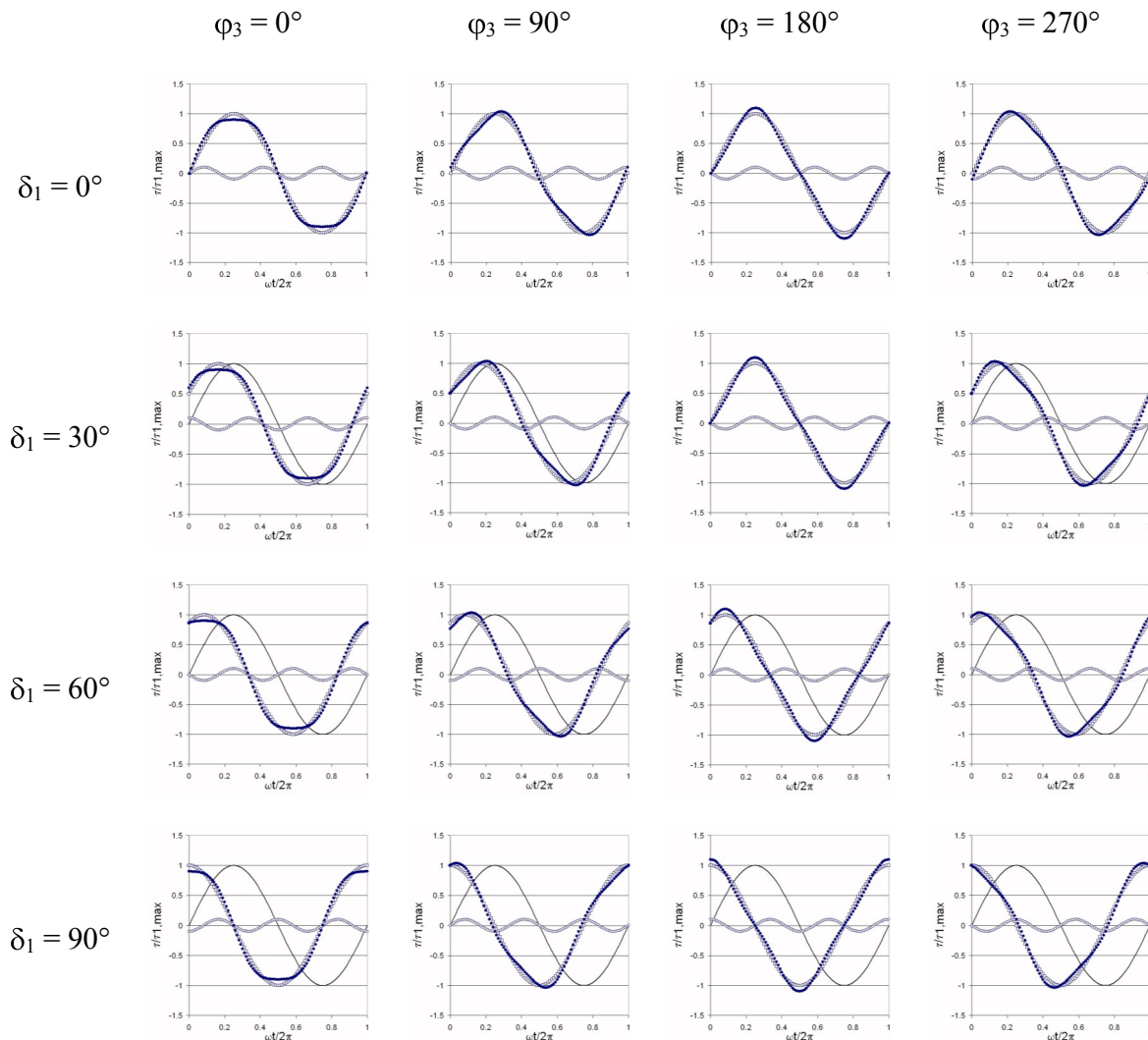


Figure 6: Waveforms of the stress for  $I_3/I_1 = 0.1$  at various phase shifts

- edge sawtooth wave)
- for  $\varphi_3 = 180^\circ$  the stress wave gets stretched vertically ( $\rightarrow$  triangle wave)
- for  $\varphi_3 = 270^\circ$  the stress wave gets distorted to the left ( $\rightarrow$  leading edge sawtooth wave)

### LISSAJOUS FIGURES

Due to the fact that the phase shift  $\varphi_3$  is referred to the fundamental, the phase angle  $\delta_1$  has no relevance for the shape of the cumulative stress curve, whereas it has an influence on the well known Lissajous figures shown in Fig. 7. Lissajous figures arise from a superposition of harmonic

oscillations as plots of in this case the stress against the strain. The shape of such a Lissajous figure depends on the frequency ratio and the phase difference at the beginning of the oscillation. For equal frequencies the figure is an ellipse with varying eccentricity depending on the phase. A line through the origin (open symbols in the row for  $\delta_1 = 0^\circ$ ) reveals the limiting linear case of purely elastic behavior, as the circle does for purely viscous behavior (open symbols in the row for  $\delta_1 = 90^\circ$ ), provided an adequate scaling of the properties with their respective amplitudes. A general rule within the linear viscoelastic region is, that the sine of the (linear viscoelastic !) phase angle  $\delta$  is the

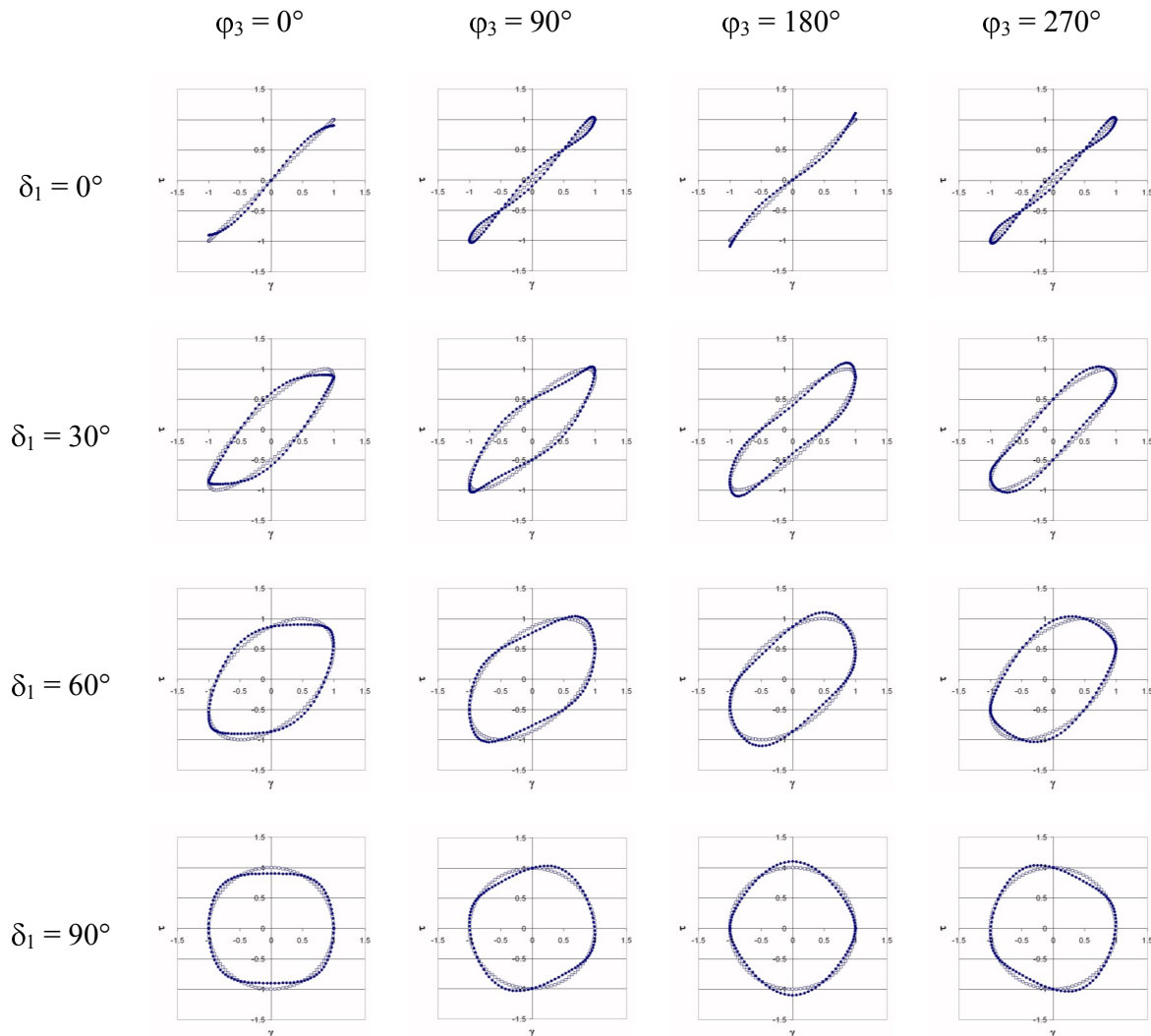


Figure 7: Lissajous-Bowditch figures for  $I_2/I_1 = 0.1$  at various phase shifts

positive value at the intersect of the Lissajous curve with the normalized strain axis.

A Lissajous figures stays unchanged with time, if the two frequencies involved have a rational ratio, i. e. can be written as a fraction of integer numbers; this is even more the case, if only odd multiples of the excitation frequency occur in the stress response. But also the in the Lissajous-Bowditch figures the effect of a third harmonics and its phase angle  $\varphi_3$  becomes evident: the „viscoelastic basic shape“ of an ellipse gets distorted vertically. As the parameter time is eliminated in this representation, the Lissajous figures do not contain further information, other than the waveforms in Fig. 6. But during an experiment it is convenient to monitor the (at first transient) Lissajous figures approaching a temporally stable pattern, in order to evaluate, whether (or when) the system has reached a quasi-steady state as far as both the amplitudes or relative intensities  $I_n/I_1$  and the phase shifts  $\varphi_n$  are concerned.

#### SIGNAL PROCESSING BY MEANS OF DISCRETE FOURIER TRANSFORMATION AND CROSS-CORRELATION

The (continuous) Fourier transformation allows for expanding any continuous, even a periodic process  $x(t)$  in a Fourier series with the continuous spectrum  $X(\omega)$ :

$$X(\omega) = \int_{-\infty}^{\infty} x(t) \exp(-i\omega t) dt \quad (7)$$

As a rheometer samples the data signals at discrete points in time, there is no continuous function  $x(t)$  for the evaluation available, only a number  $M$  of measurements  $x(m)$  of such a signal, that are each monitored after time intervals  $\Delta t$ . The highest frequency, that can be determined from such a data set is the so-called Nyquist frequency  $1/(2 \times \Delta t)$  [11], which is exactly half as large as the sampling rate [12]; the smallest frequency is given by the inverse of the

overall measuring time  $M \cdot \Delta t$ . All the discrete frequencies with

$$\begin{aligned} k \cdot \Delta f &= \frac{k}{M \cdot \Delta t} \\ \Rightarrow k \cdot \Delta \omega &= \frac{2\pi k}{M \cdot \Delta t} \quad (8) \\ \text{with } k &= 1 \dots M/2 \end{aligned}$$

contribute to the measurements  $x(m) = x(m \cdot \Delta t)$  with an amount of

$$\begin{aligned} X(k) &:= X(k \cdot \Delta \omega) \\ &= \frac{2}{M} \sum_{m=0}^{M-1} x(m) \exp\left(-i \frac{2\pi km}{M}\right) \quad (9) \end{aligned}$$

The resulting frequency spectrum is usually complex, even though the input values might be real, as the transient signal has not only an amplitude  $|X(k)|$ , but also a phase shift  $\Phi_k$  given by

$$\begin{aligned} |X(k)| &= \sqrt{X'^2 + X''^2} \\ \Phi_k &= \arctan \frac{X''(k)}{X'(k)} \quad (10) \end{aligned}$$

with

$$\begin{aligned} X'(k) &= \frac{2}{M} \sum_{m=0}^{M-1} x_r(m) \sin\left(\frac{2\pi km}{M}\right) - \underbrace{x_{im}(m) \cos\left(\frac{2\pi km}{M}\right)} \\ X''(k) &= \frac{2}{M} \sum_{m=0}^{M-1} x_r(m) \cos\left(\frac{2\pi km}{M}\right) + \underbrace{x_{im}(m) \sin\left(\frac{2\pi km}{M}\right)} \end{aligned}$$

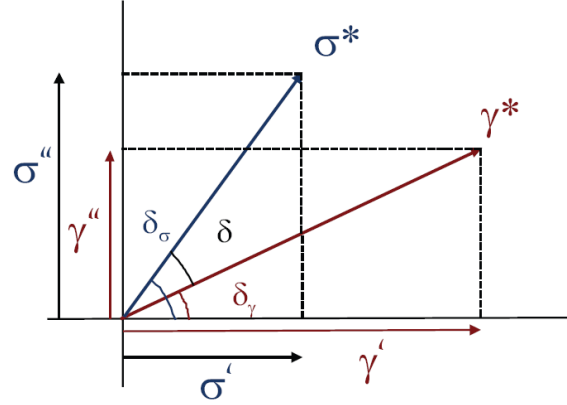
For real input values  $x(m)$  the terms between the braces just vanish. Nevertheless the effort in arithmetic operation lies in the order of  $O(M^2)$ , as both  $k$  and  $m$  run through all integer values from 1 to  $M/2$  and 0 to  $M-1$ , respectively. Therefore the so-called FFT or „Fast Fourier Transformation has been established especially for practical applications, as the arithmetic effort is „only“ of  $O(M \cdot \log M)$ . Contrary to the direct calculation, the FFT uses intermediate data that have already been calculated, thus saving computational time. One of the prerequisites for the FFT's application is the num-

ber of measurands  $M$  being a power of 2. But as the number of data points recorded during a measurement is free of choice, this is no serious restriction. Without precisely describing the literal algorithm of an FFT (this can be found in the respective literature), the efficiency of an FFT can be demonstrated with a thought example of the calculation for  $M=1000$  data points: a conventional Fourier transformation with an effort of  $O(M^2)$  needs on the order of  $1000 \cdot 1000 = 10^3 \cdot 10^3 = 10^6$ , i. e. one million calculations, whereas an FFT with  $O(M \cdot \log M)$  reduces this number down to just  $1000 \cdot \log(1000) = 1000 \cdot 3 = 3000$  ! The disadvantage of all the Fourier methods is merely that the evaluation can only be done subsequently, after all the data have been saved and stored. In the era of main memories measured in gigabytes and terabytes of hard disk sizes this should not cause any issue. As additional information the Fourier transformation delivers also values for the intensities between the higher harmonics, enabling the quantification of a signal-to-noise ratio with conclusions on the significance of the obtained relative intensities.

The cross-correlation, an alternative for the Fourier transformation, performs the evaluation virtually in real time, but gives no hint on the noise of the signal. Moreover the data set has to comply with some requirements to allow for the application of this method. This is one of the major differences between cross-correlation and the Fourier transformation, even though the mathematical operations themselves are quite similar.

In signal analysis cross-correlation is a measure of similarity of two waveforms as a function of a time-lag applied to one of them. Provided that the frequency of the measurands is known (as in the case of a stress response to a strain within the LVR), both properties, stress and strain, can be correlated with each a reference sine and a reference cosine as follows:

$$\begin{aligned}\sigma' &= \frac{2}{M} \sum_{i=0}^{M-1} \sigma_i \sin(\omega t_i) \\ \sigma'' &= \frac{2}{M} \sum_{i=0}^{M-1} \sigma_i \cos(\omega t_i) \\ \gamma' &= \frac{2}{M} \sum_{i=0}^{M-1} \gamma_i \sin(\omega t_i) \\ \gamma'' &= \frac{2}{M} \sum_{i=0}^{M-1} \gamma_i \cos(\omega t_i)\end{aligned}\tag{12}$$



$$|\gamma^*| = \sqrt{\gamma'^2 + \gamma''^2} \quad \delta_\gamma = \arctan\left(\frac{\gamma''}{\gamma'}\right)$$

$$|\sigma^*| = \sqrt{\sigma'^2 + \sigma''^2} \quad \delta_\sigma = \arctan\left(\frac{\sigma''}{\sigma'}\right)$$

$$|G^*| = \frac{|\sigma^*|}{|\gamma^*|} \quad \delta = \delta_\sigma - \delta_\gamma$$

Figure 8: Determination of the complex modulus and the (viscoelastic) phase shift from the discrete signals of stress and strain

The number  $M$  of measurands sampled each in temporal lags  $\Delta t$  has to be chosen in such a way, that the overall measuring time  $M \cdot \Delta t$  coincides with either exactly a quarter, the half or an integer multiple of the oscillation period. Meeting this requirement is finally crucial for the accuracy of an evaluation by cross-correlation.

The intensities and phase shifts of also the higher harmonics can be determined with exactly the same method of evaluation, as they contribute in the same way with a

known frequency to the response signal of the stress. Therefore the signals are similarly cross-correlated with reference waves of odd integer multiples of the excitation frequency:

$$\begin{aligned}\sigma'_n &:= \sigma'(n\omega) = \frac{2}{M} \sum_{i=0}^{M-1} \sigma_i \sin(n\omega t_i) \\ \sigma''_n &:= \sigma''(n\omega) = \frac{2}{M} \sum_{i=0}^{M-1} \sigma_i \cos(n\omega t_i)\end{aligned}\quad (13)$$

with  $n = 1$  for the fundamental and  $n = 3, 5, 7, \dots$  for the 3., 5., 7.,... higher harmonics. From these correlation either intensities and phase shifts (related to the strain) can be derived as

$$\begin{aligned}|\sigma_n| &= \sqrt{\sigma_n'^2 + \sigma_n''^2} = I(n\omega) \\ \delta_n &:= \delta(n\omega) = \arctan\left(\frac{\sigma_n''}{\sigma_n'}\right)\end{aligned}\quad (14)$$

or relative intensities  $I_n/I_1$  and harmonic phases  $i_n$  (related to the fundamental stress) as:

$$\begin{aligned}I_n / I_1 &= \frac{I(n\omega)}{I(\omega)} \\ \varphi_n &= \delta_n - n\delta_1\end{aligned}\quad (15)$$

Instead of these properties the so-called Fourier coefficients  $G_n'$  and  $G_n''$  can be determined from the intensities and phase shifts in Eq. (14), representing the stress response in the time domain:

$$\begin{aligned}\sigma(t) &= \sum_n |\sigma_n| \sin(n\omega t + \delta_n) \\ &= \sum_n |\sigma_n| \cos\delta_n \sin(n\omega t) + |\sigma_n| \sin\delta_n \cos(n\omega t) \\ &= |\gamma^*| \sum_n G_n' \sin(n\omega t) + G_n'' \cos(n\omega t)\end{aligned}\quad (16)$$

#### INTERPRETATION OF THE ADDITIONAL PARAMETERS ON EXPLAINING A MATERIAL'S BEHAVIOR

Hyaluronic acid (also called Hyaluronan) is a glycosaminoglycan, consisting of up to 100,000 repeated disaccharide units (cf. Fig.

9). Hyaluronan exhibits the ability to imbibe extremely large amounts of water related to its own mass (up to six liter water per gram). The volume required by a hydrated hyaluronan molecule can be as much as 10,000 times higher than that of the molecule itself [13]. Hyaluronan is distributed widely throughout connective, epithelial, and neural tissues and can satisfy many requirements within the human body due to the numerous and diverse chemico-physical properties. The vitreous humor of the human eye for example consists of about 98 % of water, bound to not more than 2 % of hyaluronan. Vitreous humor is the clear gel that fills the space between the lens and the retina of the eyeball of humans and other vertebrates. It is often referred to as the vitreous body or simply "the vitreous". The term "Hyaluronic acid" itself is derived from *hyalos* (Greek for vitreous) and uronic acid because it was first isolated from the vitreous humor and possesses a high uronic acid content. Water, practically incompressible, adds this property to any tissue that contains hyaluronan; this makes it of essential importance for the stability of connective tissue, especially during the phase of embryonic development, where rigid structures have not been developed sufficiently [14]. During a later stage of development, when the ability of the skin to repair itself by cell proliferation becomes less and less effective, hyaluronan once more gains of importance: this time for the external application as a cosmetic skin care product, or injected subcutaneously for filling soft tissue defects such as facial wrinkles. But also in the esthetic surgery hyaluron based products are not only used to plump up lips, but also for facial reconstruction or even arthritic treatment [14].

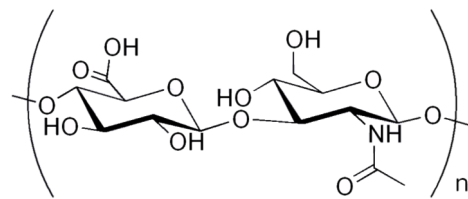


Figure 9: Structural unit of Hyaluronan

Furthermore hyaluronan can be found in the Nucleus pulposus [15], the jelly-like core of intervertebral (spinal) disks, where it aids in distributing the hydraulic pressure in all directions within each disc under compressive loads, or as a main ingredient in the synovial fluid, where it acts as a natural lubricant and thus reduces the friction between the articular cartilage and other tissues in the joint to lubricate and cushion them during movement [16]. The conditions, under which hyaluronan has to exhibit these as lubricating as damping properties are certainly hard to compare with those during a deformation within the linear viscoelastic region between the geometries of a rheometer; monitoring the material's response to extremely large deformations is required: it all comes down to LAOS.

Fig. 10 shows the result of a strain sweep on a 1 w/w-% aqueous hyaluronan solution at a frequency of 1 Hz. The linear viscoelastic region, revealed by values for storage modulus  $G'$  (●) and loss modulus

$G''$  (○), that are independent on the command strain amplitude, extends up to deformations of about 60 %; at higher strains the loss modulus decreases significantly. The storage modulus remains fairly constant up to approx. 100 %, and decreases afterwards as well. According to [1] this behavior is typical for a transition into the non-linear range of *Type I*. But already at a strain of 25 % a significant relative intensity  $I_3/I_1$  of the third harmonics (■) comes into play together with a related harmonic phase  $\varphi_3$  (s). Higher harmonics shall be neglected in this consideration.

The harmonic phase  $\varphi_3$  increases with the strain from  $-90^\circ$  ( $= 270^\circ$ ) up to  $0^\circ$  ( $= 360^\circ$ ). From these values and the cognition of Fig. 6 the conclusion is straightforward, that the waveforms of the stress response have to be distorted to the left at small strains, while getting more and more compressed with increasing strain. The proof can be found in Fig. 11; again stress and strain are plotted indistinguishably with solid lines, but as always the stress advances the strain.

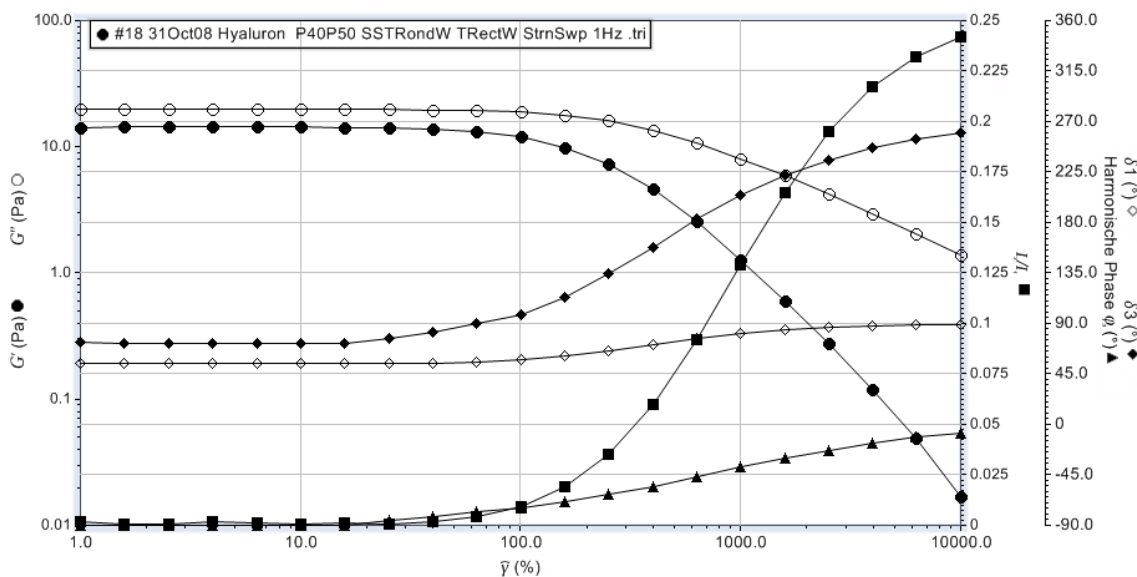


Figure 10: Dynamic moduli, relative intensity  $I_3/I_1$  and the corresponding phases from a strain sweep on a 1 w/w-%hyaluronan solution at constant frequency of 1 Hz. 40 mm on 50 mm parallel plates.

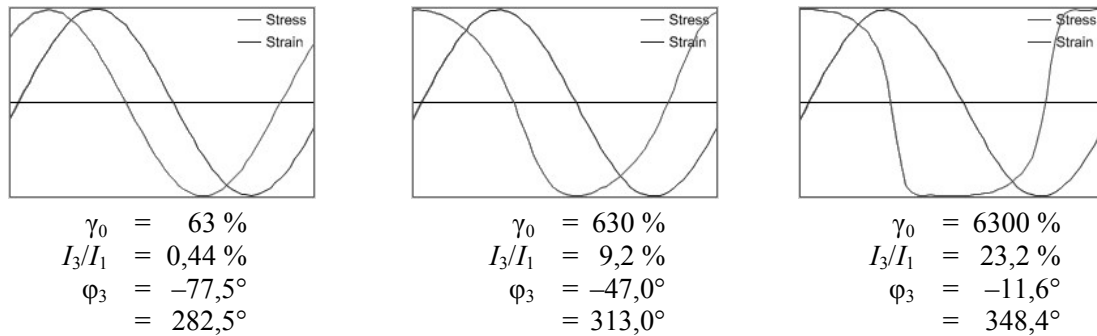


Figure 11: Waveforms of the command strain and the response stress during the strain sweep in Fig. 10 on hyaluronan .

The influence of the occurrence of higher harmonics on a material's behavior can neither be qualified, nor quantified by discussing the harmonic phase  $\varphi_3$ ; only the combination with the phase shift  $\delta = \delta_1$  ( $\diamond$ ) known from the linear viscoelasticity between the (fundamental) stress and the strain results in the phase  $\delta_3$  ( $\blacklozenge$ ) related to the deformation by rearranging Eq. (15.2):

$$\delta_3 = \varphi_3 + 3 * \delta_1 \quad (17)$$

The impact of the third higher harmonics on the material behavior varying with the magnitude of this effective phase angle  $\delta_3$  can be elucidated easily with the *LAOS circle* [17] in Fig. 12:

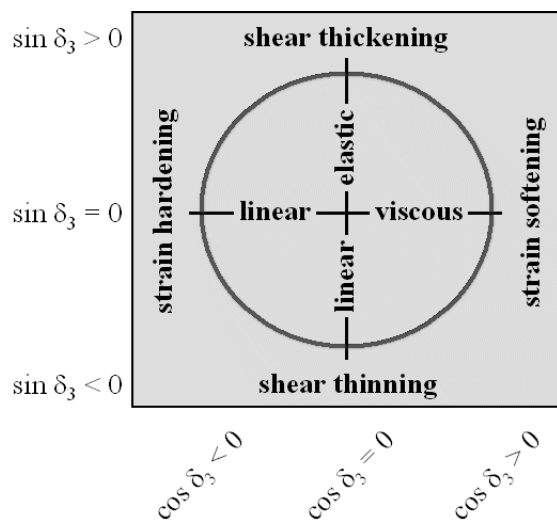


Figure 12: The LAOS circle as graphical representation of the impact of a third higher harmonics on a material's behavior

For waveforms shown in Fig. 11 the effective phase  $\delta_3$  has the following values

$$\delta_3 = 89.5^\circ$$

$$\delta_3 = 182.9^\circ$$

$$\delta_3 = 257.3^\circ$$

and allows accordingly the following interpretation for the „application“ in a knee joint:

1. At „small“ strains, just outside the LVR,  $\delta_3$  is about  $90^\circ$  and the material shows with a quasi linear-elastic behavior (comparable with the behavior within the LVR), while the **shear thickening**, that accompanies the onset of non-linearity, has a rather stabilizing effect, for example during standing still.
2. At „large“ strains of several 100 percent  $\delta_3$  is close to  $180^\circ$  and the material acts linearly viscous, though **strain hardening**, which damps in a certain way the shocks while bouncing or rope skipping.
3. At extremely large strains, that might occur during running fast,  $\delta_3$  increases up to about  $250^\circ$ , so the material doesn't exhibit these hardening or damping properties to still the same degree, but rather acts more **shear thinning**, in a sense of lubricating, to reduce the friction within the joint during movement.

## LAOS – ALSO AN EXPERIMENTAL CHALLENGE

Compared to measurement within the LVR there are some more experimental aspects to consider in LAOS experiments, which greatly influence the quality of the results. Irrespective of the magnitude of the strain amplitude the shape of the sample has to be stable and uniform. Every occurrence of edge fracture or swelling between the geometries leads to erroneous measurements in either case; but especially at large strain amplitudes these failures might occur at surprisingly low frequencies.

In the very first place the time is critical for the sample to reach a steady state. In LAOS experiments this time is much larger than in the alternative experiments with small strains. Usually 3 cycles for conditioning of the sample are considered to be sufficient in ordinary small strain experiments, but at large strain amplitudes it may take as long as 10 or more cycles, until the sample reacts with a quasi-steady state response in stress, as shown quite dramatically in Fig. 13: During the first 60 seconds the stress amplitude decreases from cycle to cycle, only in the second half of the experiment it reaches a constant value.

## SUMMARY

Conventional oscillatory experiments with comparably small deformations within the linear viscoelastic region (SAOS = Small Amplitude Oscillatory Shear) are usually performed with the goal of characterizing a material in a preferably well-defined state of equilibrium, for example to obtain information on the frequency dependent material behavior. The deformation, which is in the end imposed on the material, is very rarely even of the same order of magnitude as the strain a material is subjected to in the later application. By means of oscillatory experiments with "large" amplitude (LAOS = Large Amplitude Oscillatory Shear) at least a "rheological finger print" if not a characterization of the material can be obtained under conditions that might be a bit closer to those in reality. The representation of the furthermore non-linear behavior can be done in a graphical way

1. by means of waveforms, i. e. transient curves of stress and strain, or
2. as Lissajous-Bowditch figures, where the time is eliminated as parameter and the stress is plotted as a function of either the strain or the strain rate; a

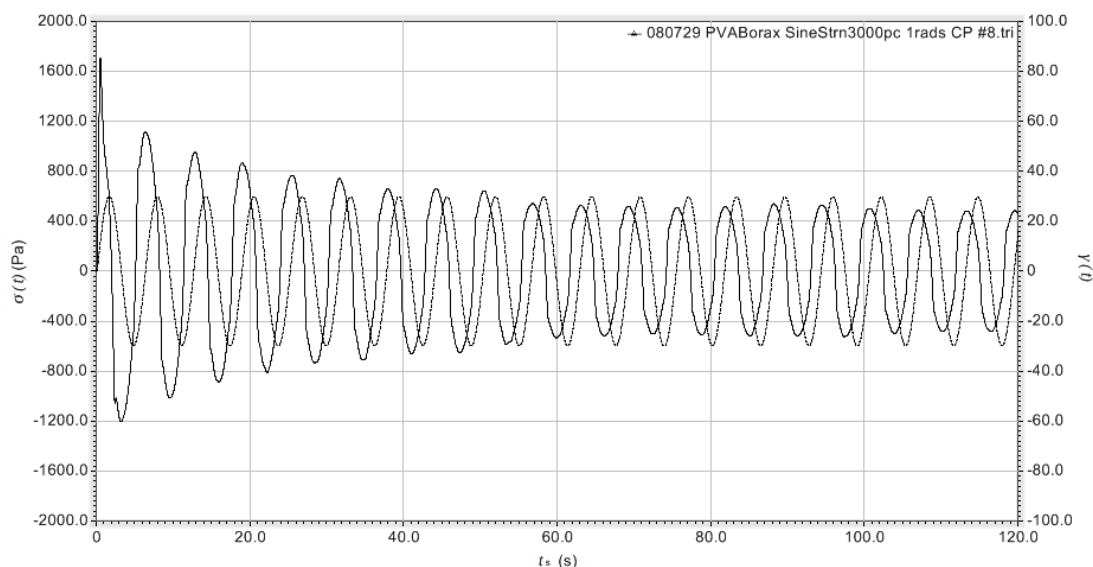


Figure 13: Transient stress  $\sigma(t)$  and strain  $\gamma(t)$  in oscillation with  $\omega = 1\text{rad/s}$  and  $|\gamma^*| = 3000\%$  on a mixture of PVA/Borax

set of these figures dependent on frequency and amplitude is then called Pipkin diagram [18],

on the other hand a quantification of the higher harmonics in the stress response on a sinusoidal deformation is achievable by indicating

3. the relative intensities, or intensity ratios  $I_n/I_1$  and the harmonic phases  $\varphi_n$  related to the fundamental stress or alternatively
4. the Fourier coefficients  $G_n'$  und  $G_n''$  corresponding to the storage modulus  $G'$  and loss modulus  $G''$  from SAOS experiments or analogously
5. the complex modulus  $|G_n^*|$  together with the phase  $\delta_n$  referred to the deformation

of in each case the  $n$ th higher harmonics. Irrespective of which representation might be individually preferred, the number of parameters will increase by two for each and every higher harmonic taken into account; as it is not unlikely, to get up to 147 higher harmonics with sufficiently large signal-to-noise ratios from a Fourier transformation [19], there is plenty of room for interpreting the influence of no fewer than 294 (!) more degrees of freedom on the behavior of a material under investigation.

## REFERENCES

- [1] Hyun, K., S. H. Kim, K. H. Ahn, S. J. Lee (2002) Large amplitude oscillatory shear as a way to classify the complex fluids. *J. Non-Newtonian Fluid Mech* **107**: 51–65
- [2] Bronstein, I. N., K. A. Semendjajew (1987) *Taschenbuch der Mathematik*, 23. Aufl., B. G. Teubner, Leipzig
- [3] Wilhelm, M., D. Maring, H. W. Spiess (1998) Fourier-Transform Rheology. *Rheol. Acta* **37**: 399–405
- [4] Wilhelm, M. (2002) *Methods and apparatus for detecting rheological properties of a material*. US patent 6,357,281
- [5] Wilhelm, M. (2003) *Methods and apparatus for detecting rheological properties of a material*. EU patent 1 000 338
- [6] Neidhöfer, T, M. Wilhelm, B. Debbaut (2003) Fourier-transform rheology experiments and finite-element simulations on linear polystyrene solutions. *J. Rheol* **47**(6):1351–1371
- [7] Kallus, S., N. Willenbacher, S. Kirsch, D. Distler, T. Neidhöfer, M. Wilhelm, H. W. Spiess (2001) Characterization of polymer dispersions by Fourier transform rheology. *Rheol Acta* **40**: 552–559
- [8] Langela M., U. Wiesner, H. W. Spiess, M. Wilhelm (2002) Microphase reorientation in block copolymer melts as detected via rheology and 2D SAXS. *Macromolecules* **35**: 3198–3204
- [9] Ewoldt, R. H., C. Clasen, A. E. Hosoi, G. H. McKinley (2006) Rheological fingerprinting of gastropod pedal mucus and bioinspired complex fluids for adhesive locomotion. *Soft. Matter* **3**: 634–643
- [10] Vittorias, I., M. Parkinson, K. Klimke, B. Debbaut, M. Wilhelm (2007) Detection and quantification of industrial polyethylene branching topologies via Fourier-transform rheology, NMR and simulation using the Pom-pom model. *Rheol Acta* **46**: 321–340
- [11] Shannon, C. E. (1949) Communication in the presence of noise. *Proc. IRE* **37**(1): 10–21. Nachdruck in: *Proc. IEEE* **86**(2), 1998
- [12] Nyquist, H. (1928) Certain topics in telegraph transmission theory. *Trans. AIEE* **47**:617–644. Nachdruck in: *Proc. IEEE* **90**(2), 2002
- [13] <http://de.wikipedia.org/wiki/Glykosaminoglykane>
- [14] <http://de.wikipedia.org/wiki/Hyalurons%C3%A4ure>
- [15] [http://flexikon.doccheck.com/Nucleus\\_pulposus](http://flexikon.doccheck.com/Nucleus_pulposus)
- [16] <http://flexikon.doccheck.com/Synovia>

- [17] Franck, A. J., M. Nowak (2008) Non-Linear Oscillation Testing with a Separate Motor Transducer Rheometer. *XV<sup>th</sup> Int. Congr. Rheol.*, Monterey, CA, USA
- [18] Pipkin, A. C (1972) *Lectures on Viscoelasticity Theory* (Applied Mathematical Sciences, Vol. 7), Springer-Verlag, Berlin/Heidelberg/New York
- [19] Wilhelm, M. (2008) *New developments in mechanical characterization of materials: FT-Rheology*. Talk on the occasion of the ARES-G2 presentation in Karlsruhe on October, 14<sup>th</sup> 2008, organized by TA Instruments, Germany.



Figure 14: A Tsunami – yet another wave with extremely large amplitude